Istanbul Bridge Conference
August 11-13, 2014
Istanbul, Turkey

BUFFETING RESPONSE OF THE IZMIT BAY BRIDGE: NUMERICAL AND EXPERIMENTAL RESULTS

G. Diana[1], D. Rocchi[1], T. Argentini[1]

ABSTRACT

A numerical-experimental comparison of the aeroelastic response of the Izmit Bay Bridge under wind action is presented. Wind tunnel tests were carried on in the wind tunnel of Politecnico di Milano on a 1:220 scale aeroelastic model, both in smooth and turbulent flow conditions, to investigate the aeroelastic stability and the buffeting response of the structure at in-service and in-construction stages.

The experimental results are compared with the output of numerical simulations obtained using a linear aerodynamic force model. The validated model can be used to investigate the operating condition of the bridge considering different wind scenarios.

[1] Department of Mechanical Engineering, Politecnico di Milano, Milan, Italy

G. Diana, D. Rocchi, T. Argentini. Buffeting Response of the Izmit Bay Bridge: Numerical and Experimental Results. *Proceedings of the Istanbul Bridge Conference*, 2014.

Buffeting response of the Izmit Bay Bridge: numerical and experimental results

G. Diana[1], D. Rocchi[1], T. Argentini[1]

ABSTRACT

A numerical-experimental comparison of the aeroelastic response of the Izmit Bay Bridge under wind action is presented. Wind tunnel tests were carried on in the wind tunnel of Politecnico di Milano on a 1:220 scale aeroelastic model, both in smooth and turbulent flow conditions, to investigate the aeroelastic stability and the buffeting response of the structure at in-service and in-construction stages.

The experimental results are compared with the output of numerical simulations obtained using a linear aerodynamic force model. The validated model can be used to investigate the operating condition of the bridge considering different wind scenarios.

Introduction

The static and dynamic behavior of long span bridge under wind actions is a fundamental aspect that allows one to assess the performance of the structure and the effectiveness of its design. The accurate study of bridge aerodynamics is very important since several wind-structure interaction problems may occur: vortex-induced vibrations, aeroelastic instabilities (divergence, galloping, flutter), or excessive buffeting vibrations.

Numerical studies (e.g. [1,2,3,4,5,6]), performed in the preliminary and final stages of the design of a long span bridge, must be validated against wind tunnel tests on scale models before the final go for the project. In the light of these considerations, this paper presents an experimental–numerical comparison of the buffeting response of the Izmit Bay Bridge in its in-service configuration.

Buffeting response is always an issue that must be investigated for a long span bridge for in-service condition and during the construction. In order to ensure the aerodynamic stability of the bridge, and acceptable vibration levels in all its configurations, an extensive wind tunnel test campaign with aeroelastic bridge models was carried out, and results are compared in this paper with a numerical simulation.

Wind tunnel tests are able to reproduce the complex wind structure-interaction occurring between a turbulent wind and all the bridge parts. The reliability of wind tunnel results depends on the correct modeling of the structural dynamics (mode shapes and frequencies) and of the incoming wind turbulent characteristics. They are able to highlight the aeroelastic effects (frequency shifting, aerodynamic damping, etc…), but are not sufficient for the final design of the structure. On the other hand numerical simulations need to be validated, in order to be used as a design tool to investigate the complex aeroelastic effects.

[1]Department of Mechanical Engineering, Politecnico di Milano, Milan, Italy

G. Diana, D. Rocchi, T. Argentini. Buffeting Response of the Izmit Bay Bridge: Numerical and Experimental Results. *Proceedings of the Istanbul Bridge Conference*, 2014.

The Izmit Bay Bridge

The Izmit Bay Bridge (IBB) is a three spans suspension bridge with a main span of 1550 m and two side spans of 566 m. Each tower is a 235.43 m high steel structure having two crossbeams connecting two tower legs at the middle level and at the top. The tower foundations are placed on the gravel bed, at 40 m below water level. The main cables are deviated at the side span piers and anchored at the cable anchor blocks. The deck is a classical streamed line single box (characterized by a three-lane dual carriageway with no railway), 31.5 m wide and 4.75 m deep, having 2.8 m wide inspection walkway on both sides. The general arrangement of the bridge is shown in Fig. 1, while the deck cross-section is shown in Fig.2.

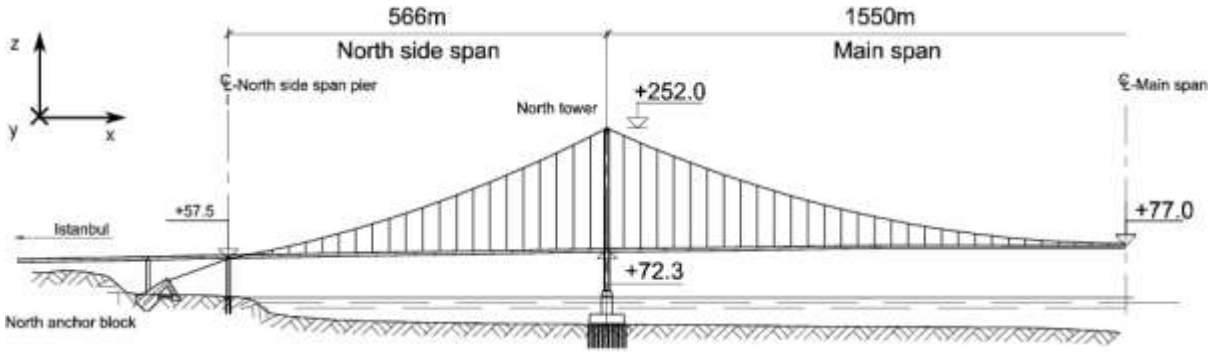

Figure 1. General arrangement of the IBB

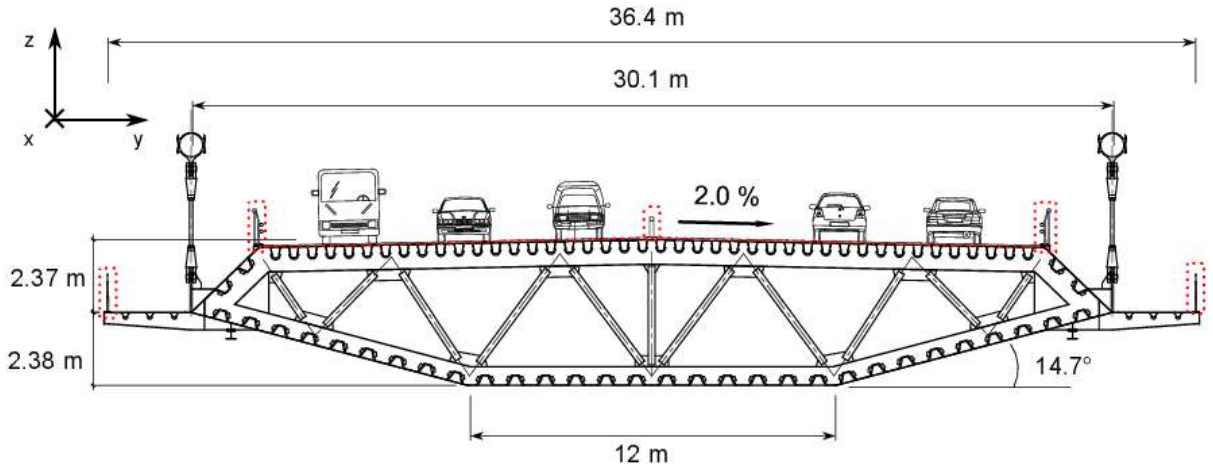

Figure 2. Typical cross sections overall dimensions

Experimental Aeroelastic Tests

Aeroelastic tests were performed on an aeroelastic model of the full bridge in the Boundary Layer Wind Tunnel of Politecnico di Milano (see Figure 3). The model was realized in a geometrical scale $\lambda = 1:220$, using Froude similarity.

Both deck and towers consist of an internal aluminum spine and an external covering made of modeling foam. The former is designed to represent the scaled elastic properties of the real structure, while the latter reproduces the external aerodynamic shape and it accounts for mass distribution. The external covering consists of a series of rigid modules locally connected to

the internal spine by screws or structural glue. A gap of 1–2 mm is left between each modules. The inertial properties and the mass of the structure, that vary along the bridge axis, are tuned by the addition of lumped lead masses in each module, in order to achieve the target mass and moments of inertia. The inertial properties of each module is singularly calibrated. At the tower top, the mass of the saddle is modeled with lumped elements reproducing the angle between the cable and the tower. Axial springs allow to correctly reproduce the axial stiffness of the main cables. Lumped cylindrical masses are positioned along the cables to reproduce both the mass and the aerodynamic properties of the cable in terms of drag, taking into account Reynolds number discrepancy between model and full scale. A detailed description of the aeroelastic model is given in [7].

The turbulent boundary layer characteristics are simulated using spires and artificial roughness in the wind tunnel. An example of comparison of target and achieved characteristics in the wind tunnel is given in Fig 4.

Figure 3. The full bridge aeroelastic model in the boundary layer wind tunnel (left) and a detail of one construction stage analyzed (right)

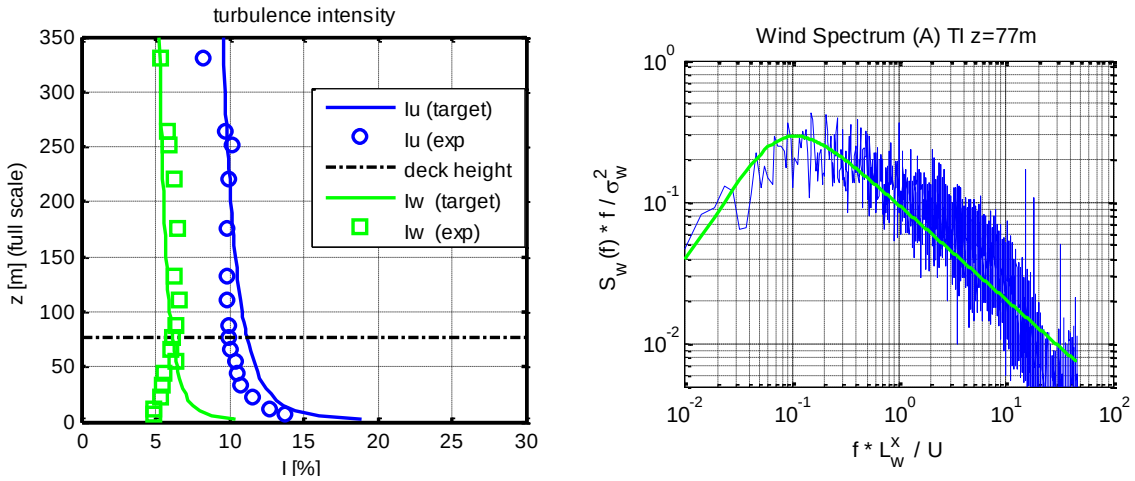

Figure 4. Example of target and experimental turbulence characteristics of the boundary layer: vertical profile of turbulence intensities (u and w) and spectrum of vertical wind component w

Numerical simulation of buffeting response

Numerical buffeting response simulation is performed according to the scheme reported in Fig 5: a beam FEM model of the complete bridge is used to simulate the dynamics of the structure; aerodynamic forces are applied to the structure using a sectional approach. For each section aeroelastic and buffeting forces are computed using experimental aerodynamic coefficients and digitally simulated incoming turbulent wind.

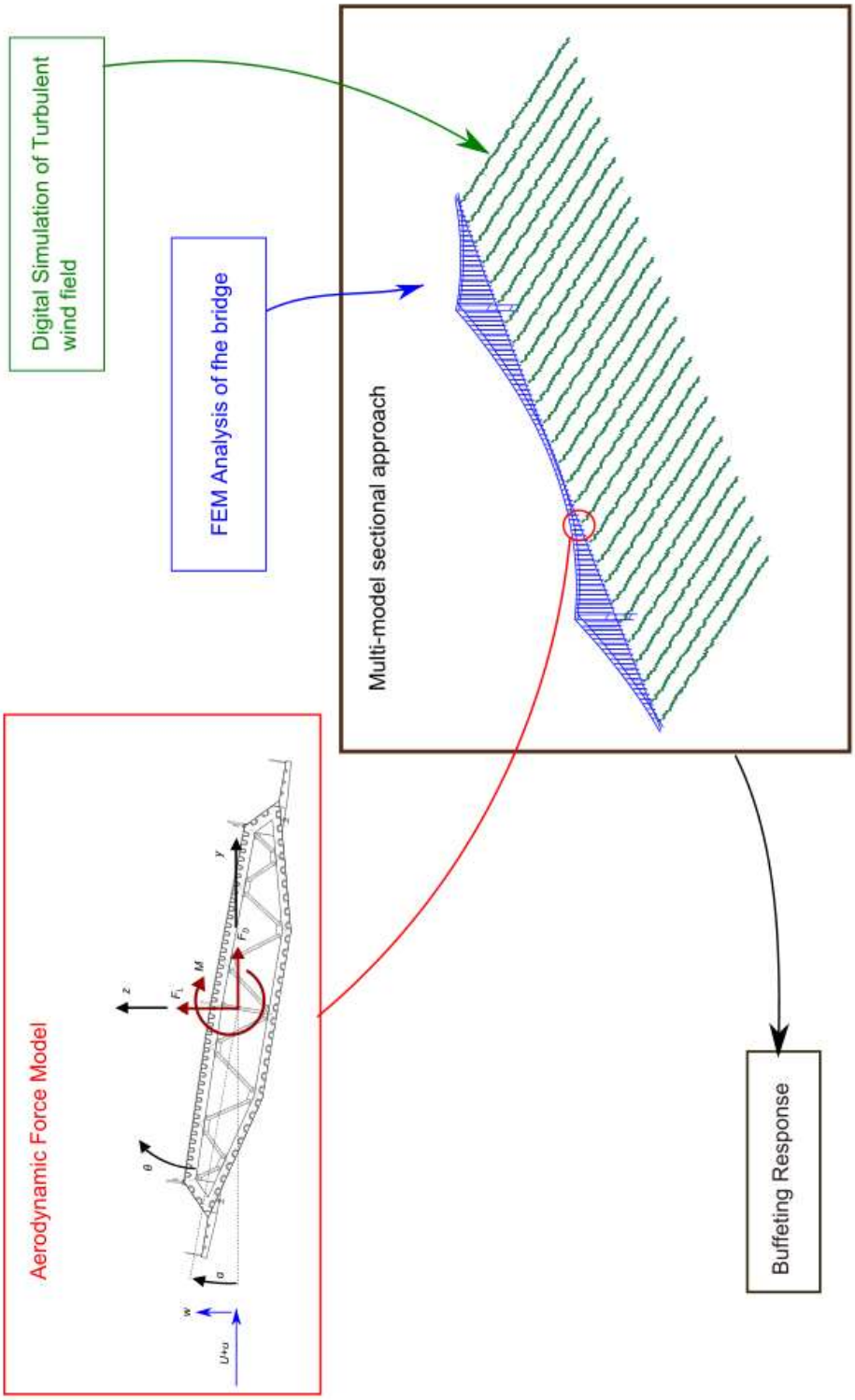

Figure 5. Example of target and experimental turbulence characteristics of the boundary

The aeroelastic buffeting response is simulated using a multi-modal approach on the complete scheme of the bridge. To define the aerodynamic forces the deck is divided into several rigid sections subjected to a bi-dimensional fluid-structural interaction that is a widely accepted hypothesis for slender structures. The mode shapes, the natural frequencies and the modal parameters of the bridge (modal mass and stiffness) in still air are computed through a finite elements scheme of the structure.

Adopting the modal approach, the dynamics of the structure can be written as:

$$\left[M_s^*\right]\underline{\ddot{q}}+\left[C_s^*\right]\underline{\dot{q}}+\left[K_s^*\right]\underline{q}=\left[\Phi\right]^T\underline{F}_{aero}=\underline{Q}_{aero} \tag{1}$$

where $\underline{q}$ is the vector of the modal coordinates; $\left[M_s^*\right]$, $\left[C_s^*\right]$ and $\left[K_s^*\right]$ are the structural inertial, damping, and stiffness modal matrices of the system; $\underline{Q}_{aero}$ is the vector of the lagrangian components of the external aerodynamic forces ($\underline{F}_{aero}$).

The external aerodynamic forces ($\underline{F}_{aero}$) are computed as the sum of three different effect, namely:

$$\underline{F}_{aero}=\underline{F}_{ST}+\underline{F}_{se}+\underline{F}_{buff} \tag{2}$$

Where $\underline{F}_{ST}$ are the stationary aerodynamic forces, $\underline{F}_{se}$ the self-excited, and $\underline{F}_{buff}$ the buffeting forces. Aerodynamic forces are applied only to the deck.

Stationary aerodynamic coefficients

The steady aerodynamic coefficients for drag, lift and moment forces acting on the j-th deck section are reported in Fig 6. The definition of the forces per unit length is:

$$\underline{F}_{ST}=\frac{1}{2}\rho V^2 B\begin{bmatrix} C_D \\ C_L \\ BC_M \end{bmatrix} \tag{3}$$

where B is the deck chord, V the mean wind velocity, and rho the air density.

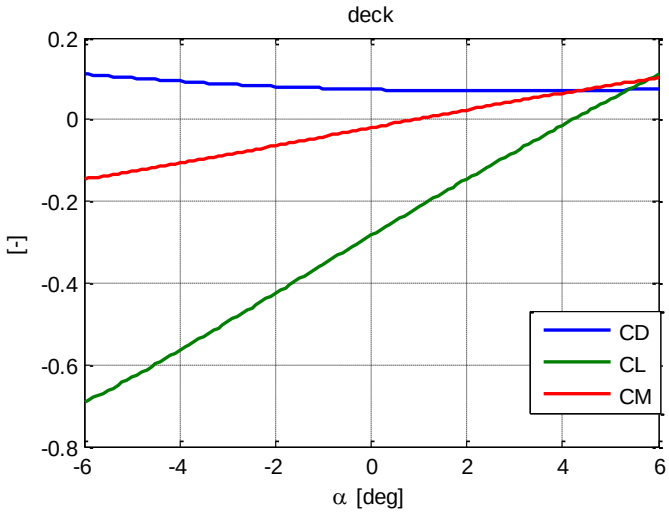

Figure 6. Stationary aerodynamic coefficients

Self-excited wind loads

The self-excited unsteady aerodynamic terms of drag, lift and moment acting on the j-th deck section (D_j, L_j, and M_j in Figure 4) are modeled using the Flutter Derivatives coefficients, that were measured with dedicated forced motion tests at the wind tunnel of Politecnico di Milano (see Fig 5). The self-excited forces acting on the generic j-th section are defined, according to the Politecnico di Milano convention (see [5]), as:

$$\begin{bmatrix} D_j \\ L_j \\ M_j \end{bmatrix}_{aero} = \left[m^*_{aero,j}\right]\begin{Bmatrix} \ddot{y}_j \\ \ddot{z}_j \\ \ddot{\theta}_j \end{Bmatrix} + \left[c^*_{aero,j}\right]\begin{Bmatrix} \dot{y}_j \\ \dot{z}_j \\ \dot{\theta}_j \end{Bmatrix} + \left[k^*_{aero,j}\right]\begin{Bmatrix} y_j \\ z_j \\ \theta_j \end{Bmatrix} \tag{4}$$

where y_j, z_j and θ_j are respectively the lateral, vertical and torsional displacements of the j-th section, $\left[m^*_{aero,j}\right]$,$\left[c^*_{aero,j}\right]$ and $\left[k^*_{aero,j}\right]$ are the aerodynamic matrices related to the j-th section, expressed, per unit length, as:

$$\left[m^*_{aero,j}\right] = \frac{1}{2}\rho V_j^2 B \begin{bmatrix} p_6^* \frac{\pi B}{2V_j^2} & p_4^* \frac{\pi B}{2V_j^2} & 0 \\ h_6^* \frac{\pi B}{2V_j^2} & h_4^* \frac{\pi B}{2V_j^2} & 0 \\ a_6^* \frac{\pi B^2}{2V_j^2} & a_4^* \frac{\pi B^2}{2V_j^2} & 0 \end{bmatrix} \quad \left[c^*_{aero,j}\right] = \frac{1}{2}\rho V_j^2 B \begin{bmatrix} -p_5^* \frac{1}{V_j} & -p_1^* \frac{1}{V_j} & -p_2^* \frac{B}{V_j} \\ -h_5^* \frac{1}{V_j} & -h_1^* \frac{1}{V_j} & -h_2^* \frac{B}{V_j} \\ -a_5^* \frac{B}{V_j} & -a_1^* \frac{B}{V_j} & -a_2^* \frac{B^2}{V_j} \end{bmatrix}$$

$$\left[k^*_{aero,j}\right] = \frac{1}{2}\rho V_j^2 B \begin{bmatrix} 0 & 0 & p_3^* \\ 0 & 0 & h_3^* \\ 0 & 0 & a_3^* B \end{bmatrix} \tag{5}$$

being V_j the mean wind speed for the j-th section, B the bridge deck chord (used as reference length), and a_i^*, h_i^* and p_i^* with $i = \{1 \div 6\}$ the flutter derivative coefficients. a_i^*, h_i^* and p_i^* are function both of the reduced velocity ($V_j^* = V_j / (fB)$, being f the motion frequency), and of the angle of attack α_j, that is function of the mean wind speed itself, being related to the deflected position reached under the mean wind speed stationary load.

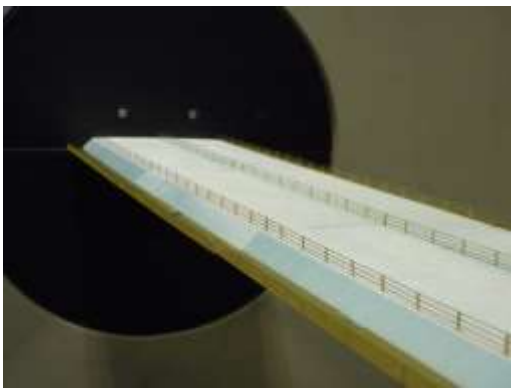

Figure 7. Experimental setup for measuring flutter derivatives and static coefficients (in 1:220 scale)

Table 1. Main flutter derivatives for the IBB bridge.

V*	a2	a3	h3
4	0.17	0.85	4.0
6	0.22	0.85	3.9
7	0.3	0.85	3.9

The most relevant flutter derivatives coefficients as a function of the reduced velocity for the IBB are reported in Table 1. A detailed explanation of the self-excited wind loads simulation is given in [**2**].

Buffeting forces

Buffeting forces are due to the incoming turbulent wind. They are defined through the so-called aerodynamic admittance functions as:

$$\begin{Bmatrix} D_j \\ L_j \\ M_j \end{Bmatrix} = \frac{1}{2}\rho V_j^2 B \begin{bmatrix} \chi_{D-u}\left(V^*,\alpha\right) & \chi_{D-w}\left(V^*,\alpha\right) \\ \chi_{L-u}\left(V^*,\alpha\right) & \chi_{L-w}\left(V^*,\alpha\right) \\ B\chi_{M-u}\left(V^*,\alpha\right) & B\chi_{M-w}\left(V^*,\alpha\right) \end{bmatrix} \begin{Bmatrix} \frac{u}{V_j} \\ \frac{w}{V_j} \end{Bmatrix} \tag{6}$$

χ are the aerodynamic admittance functions (dependent upon both of the reduced velocity and of the angle of attack α_j**)**, while u and w are the turbulent horizontal and vertical components of the turbulent wind field. Admittance functions can be measured with dedicated wind tunnel tests [**3**], or alternatively quasi-steady theory can be used.

The simulation of the turbulent wind field is done according the procedure outlined in [7] and [9]. It requires as input parameters the definition of the spectra of the turbulence, the integral length scales, the turbulence intensities, the spatial coherence functions, wind speed profile.

Numerical-Experimental comparison of buffeting response

Numerical results are compared with experimental ones in Figures 8—11. The comparison is proposed in terms of PSD of vertical and torsional acceleration at mid-span and quarter span, for a wind velocity range between 30 and 60 m/s full scale, at deck height.

In Figures 9 and 11 it is clearly visible the frequency shift of the first and second torsional modes, due to the a^*_3 coefficient (aerodynamic torsional stiffness). This coefficient is constant and has a value of 0.85 (see Table 1) in the range of reduced velocities for these modes ($4<V^*<7$). Therefore, the aerodynamic torsional stiffness depends only on V^2 (see Eq. 5). The value is lower than the quasi-steady one, which can be inferred by the slope of the C_M coefficient (equal to 1.2). Thus, specific wind tunnel tests are necessary to measure the flutter derivatives.

In general, the distribution of the energy input of the turbulent wind is well reproduced in the response of the structure, especially for the lower frequency modes that are better reproduced by the aeroelastic model, as it was shown by modal identification performed on wind tunnel models ([7]).

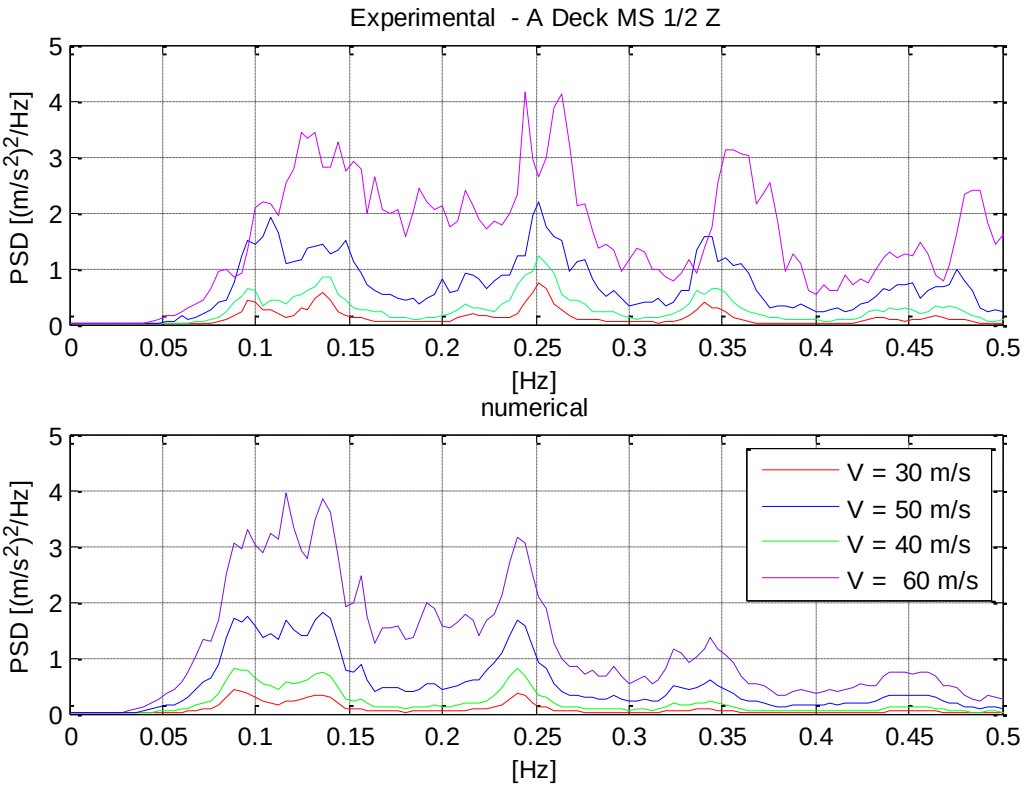

Figure 8. PSD of vertical acceleration at mid-span for several wind speeds: experimental vs. numerical

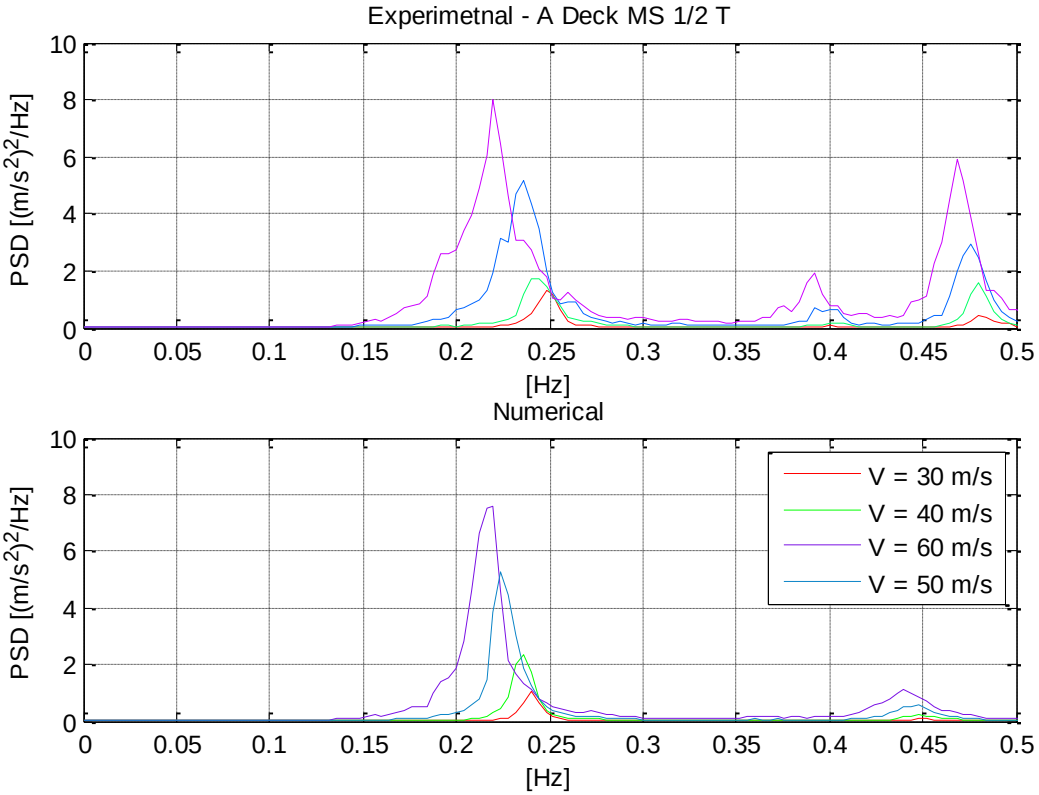

Figure 9. Figure 6. PSD of torsional acceleration at deck edge at mid-span for several wind speeds: experimental vs. numerical

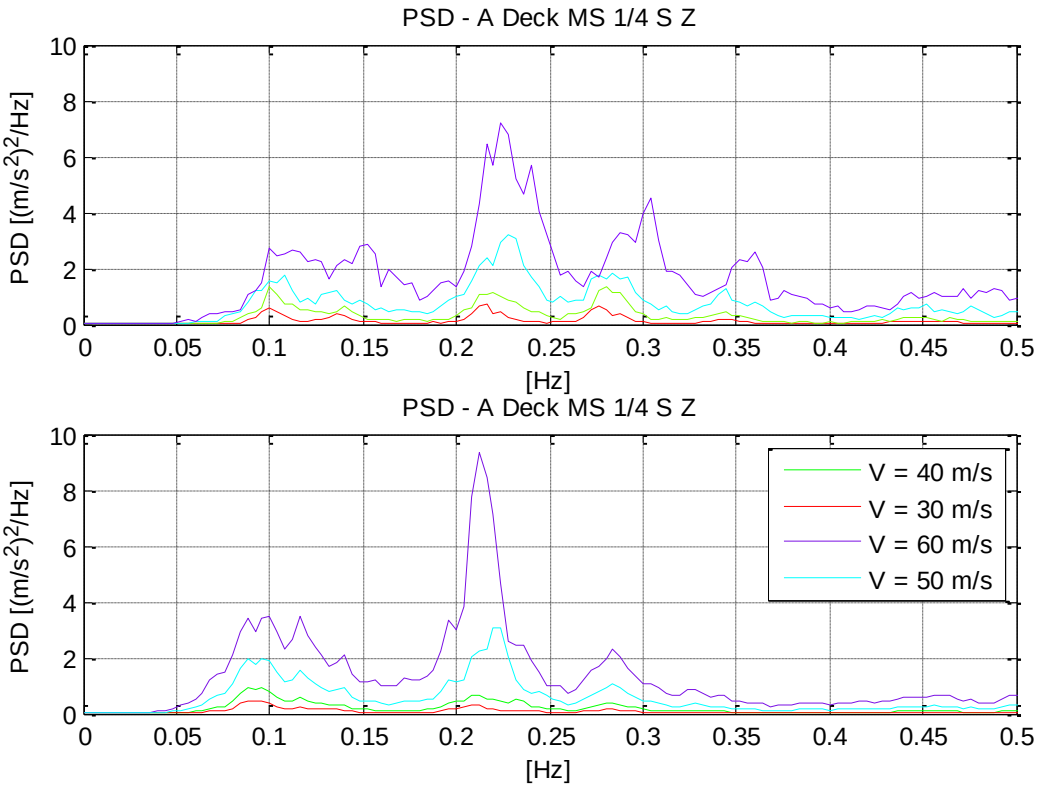

Figure 10. PSD of vertical acceleration at quarter-span for several wind speeds: experimental vs. numerical

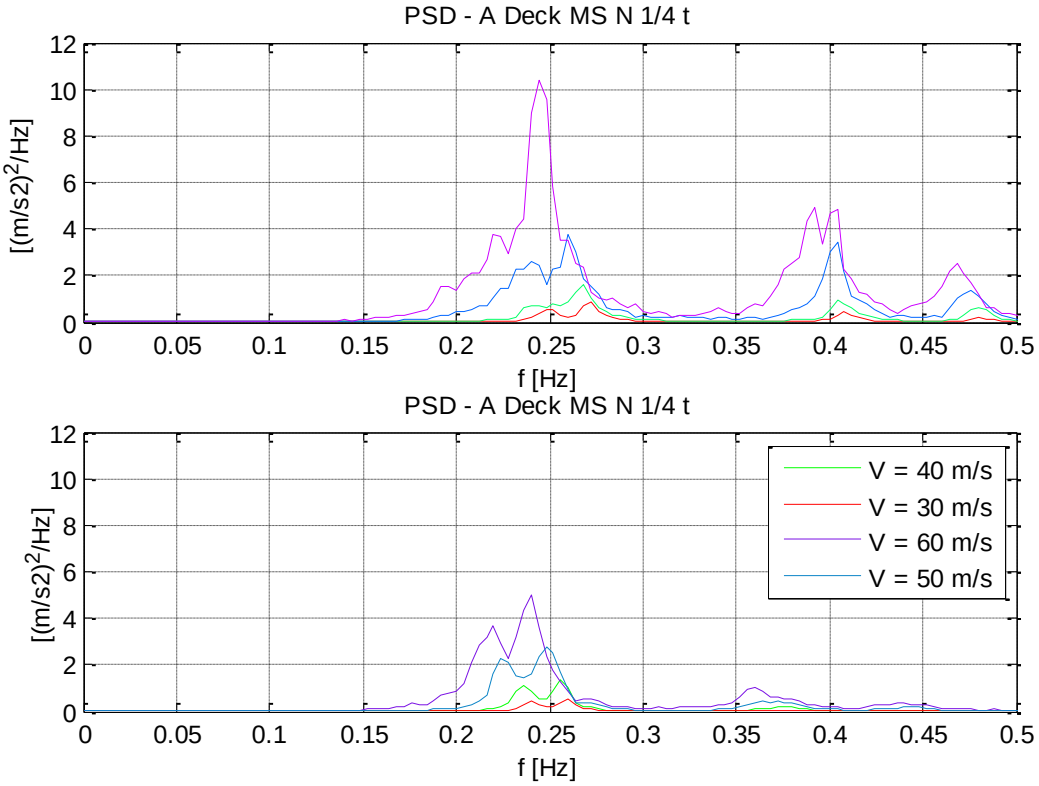

Figure 11. Figure 6. PSD of torsional acceleration at deck edge at quarter-span for several wind speeds: experimental vs. numerical

Conclusions

The validation of a linear modeling of the wind-bridge interaction for the IBB has been presented. The comparison between the wind tunnel results and the numerical simulations allowed to investigate the aeroelastic effects on the first vibration modes of the bridge, in particular the torsional frequency shift and the coupling between homologous vertical and torsional modes. The simulations highlighted the need to consider the aeroelastic coefficients dependency on the reduced velocity, in order to obtain a correct reproduction of the aeroelastic effects shown in the wind tunnel tests. Moreover, to achieve a satisfactory comparison, a reproduction of the wind tunnel wind field has been used.

The validated numerical approach can be used to investigate a large number of wind scenarios to assess the behavior of the structure in full-scale operating conditions and to compute wind loads that are difficult to measure with aeroelastic models (e.g. stress and deformations).

Acknowledgements

The experimental campaign was done in cooperation with COWI A/S.

References

1. Argentini, T.; Belloli, M.; Fossati, F.; Rocchi, D. & Villani, M. Experimental and numerical analysis of the dynamic response of cable-stayed bridge: vortex induced vibrations and buffeting effects, ICWE2011, 2011
2. Argentini, T.; Pagani, A.; Rocchi, D. & Zasso, A., Monte Carlo analysis of total damping and flutter speed of a long span bridge: Effects of structural and aerodynamic uncertainties Journal of Wind Engineering and Industrial Aerodynamics, Vol. 128, pp. 90-104, 2014
3. Diana, G.; Rocchi, D. & Argentini, T. An experimental validation of a band superposition model of the aerodynamic forces acting on multi-box deck sections, Journal of Wind Engineering & Industrial Aerodynamics, Vol. 113, pp. 40-58, 2013.
4. Diana, G.; Rocchi, D.; Argentini, T. & Muggiasca, S., Aerodynamic instability of a bridge deck section model: Linear and nonlinear approach to force modelling. Journal of Wind Engineering and Industrial Aerodynamics, Vol. 98, pp. 363-374, 2010
5. Zasso, A.; Stoyanoff, S.; Diana, G.; Vullo, E.; Khazem, D.; Pagani, K. S. A.; Argentini, T.; Rosa, L. & Dallaire, P. O., Validation analyses of integrated procedures for evaluation of stability, buffeting response and wind loads on the Messina Bridge. Journal of Wind Engineering & Industrial Aerodynamics, Vol. 122, pp. 50-59, 2013
6. Argentini, T.; Diana, G.; Larsen, A.; Pagani, A.; Portentoso, M.; Somaschini, C. & Yamasaki, Y. Comparisons between wind tunnel tests on a full aerolastic model and numerical results of the Izmit Bay Bridge. 6th European African Conference on Wind Engineering, 2013
7. Diana, G.; Yamasaki, Y.; Larsen, A.; Rocchi, D.; Giappino, S.; Argentini, T.; Pagani, A.; Villani, M.; Somaschini, C. & Portentoso, M. Construction stages of the long span suspension Izmit Bay Bridge: wind tunnel test assessment. Journal of Wind Engineering & Industrial Aerodynamics, 2013,123, 300-310
8. Ding, Q.; Zhu, L. & Xiang, H.Simulation of stationary Gaussian stochastic wind velocity field Wind and Structures, An International Journal, 2006, 9, 231-243
9. Deodatis, G.Simulation of ergodic multivariate stochastic processes. Journal of Engineering Mechanics, 1996, 122, 778-787